The positive exchange bias property with hopping switching behavior in van der Waals magnet FeGeTe

2D Materials

PAPER

RECEIVED
10 September 2021

REVISED
29 November 2021

ACCEPTED FOR PUBLICATION
21 December 2021

PUBLISHED
5 January 2022

The positive exchange bias property with hopping switching behavior in van der Waals magnet FeGeTe

Shaojie Hu[1,2,*], **Xiaomin Cui**[3], **Zengji Yue**[4], **Pangpang Wang**[5], **Lei Guo**[6], **Kohei Ohnishi**[1], **Xiaolin Wang**[4] and **Takashi Kimura**[1,*]

[1] Department of Physics, Kyushu University, 744 Motooka, Fukuoka 819-0395, Japan
[2] Center for Spintronics and Quantum Systems, State Key Laboratory for Mechanical Behavior of Materials, School of Materials Science and Engineering, Xi'an Jiaotong University, Xi'an, Shaanxi 710049, People's Republic of China
[3] School of Physical Science and Technology, Northwestern Polytechnical University, Xi'an, 710072, People's Republic of China
[4] Institute for Superconducting & Electronic Materials, ARC Centre for Future Low-Energy Electronics Technologies, University of Wollongong, Wollongong, NSW 2500, Australia
[5] Institute of Systems, Information Technologies and Nanotechnologies (ISIT), Fukuoka 819-0388, Japan
[6] School of Physics, Southeast University, Nanjing 211189, People's Republic of China
[*] Authors to whom any correspondence should be addressed.

E-mail: hu.shaojie@phys.kyushu-u.ac.jp, shaojiehu@mail.xjtu.edu.cn and t-kimu@phys.kyushu-u.ac.jp

Keywords: exchange bias effect, FeGeTe, 2D ferromagnet

Abstract

The magnetic exchange bias (EB) effect is one of the representative interlayer magnetic coupling phenomena and is widely utilized in numerous technological applications. However, its mechanism is still elusive even in a simple magnetic bilayered system because of the complex interface magnetic orders. Van der Waals (vdW) layered magnetic materials may provide an essential platform for deeply understanding the detailed mechanism of the EB owing to its ideal interface structure. Here we first observed the positive exchange-biased anomalous Hall effect with a hopping switching behavior in the FeGeTe vdW nano-flakes. After systemically studying the cooling field dependence properties of the EB effect, we propose that the coexistence of stable and frustrated surface magnetization of the antiferromagnetic (AFM) phase will modify the total interface coupling energy density between the ferromagnetic and AFM phases. This model could provide a consistent description for such unusual EB effect based on microspin simulation.

1. Introduction

Exchange bias (EB) or exchange anisotropy effect [1], arising from interface magnetic coupling, is an integral part of fundamental science and device application in the field of spintronics. The most general EB is achieved between different magnetic phases, such as antiferromagnetic-ferromagnetic (AFM/FM) [2–4], ferrimagnetic (FRM)-AFM [5], FRM-FRM [6] and FRM-FM [7–9] material systems. Besides, the EB behavior can also be realized by the indirect exchange coupling, Ruderman–Kittel–Kasuya–Yosida (RKKY) coupling, which is the weak magnetic coupling between AFM and FM through a nonmagnetic (NM) spacer (AFM-NM-FM) [10–12]. It should also be noted that the RKKY-like exchange coupling can also induce EB in a spin glass/FM bilayer system [13–18]. The coupling between the topological properties and magnetic texture can also induce strong exchange biased effect in the complex magnetic disorder materials [19, 20].

With the emergence of van der Waals (vdW) materials during the past decades, the vdW ferromagnets, including intrinsic FM and AFM orders, have been discovered very recently [21–24]. The two-dimensional vdW magnetic materials provide an ideal platform to study magnetic coupling phenomena deeply. Of particular interest is the EB effect, which is crucial to understand magnetic coupling in vdW layers. The EB effect has been studied in the artificial AF/FM vdW structures, such as CrI_3/Fe_3GeTe_2, $Fe_3GeTe_2/CrPS_4$ $Fe_3GeTe_2/FePS_3$, $Fe_3GeTe_2/MnPX$ and $Fe_3GeTe_2/IrMn$ [25–30]. All those are the direct magnetic coupling at the interface of AFM/FM. Interestingly, the exchange-biased effect was also found in the vdW ferromagnet FeGeTe (FGT) nanoflakes

itself [31, 32]. They all mentioned that the coupling between the AFM phase and FM phase is the key point. But the AFM coupling mechanism is still a controversy in this materials because of the complex competition effects, such as Ising ferromagnetism and Kondo screening effect inner-layer, RKKY interaction and Dzyaloshinskii–Moriya interaction between interlayer [33–35]. Here we experimentally observed a positive exchange-biased anomalous Hall effect (AHE) in the FeGeTe nano-flakes. Such unconventional EB also shows a nontrivial training effect. After we systemically studied the cooling field dependence of exchange-biased AHE, we propose that unconventional exchange-biased AHE is induced by the coexistence of stable and frustrated surface magnetization of the AFM phase.

2. Method

High-quality FeGeTe single crystals were grown by the chemical vapor transport method using iodine (I_2) as a transport agent. Briefly, high-purity stoichiometric amount powders (1 g) of Fe, Ge, and Te, together with 10 mg ml^{-1} iodine, are sealed in a quartz tube as the starting materials. The bulk crystal was growth in a two-zone furnace between 750 °C (source) and 700 °C (sink) for one week. Then the thin FGT flakes were obtained by the mechanical exfoliation method on the SiO_2/Si substrate in an argon atmosphere glove box. Subsequently, the photo-resist was spin-coated on the substrate to prevent the oxidation of FGT flakes. After the preparation of thin FGT flakes, we fabricated the cloverleaf structure to evaluate the electric transport properties of the FGT flakes. The electrodes of Ti/Cu were fabricated by using the electron beam lithography and wet lift-off process. Here, the 5 nm Ti was deposited in the ultra-high vacuum electron beam evaporator to get better adhesion. Then 100 nm Cu was deposited by using Joule evaporator in the same chamber without breaking the vacuum. After that, we etched the excess part of the thin FGT flakes by argon ion-beam etching to get the standard cloverleaf structure. The scanning electron microscopy (SEM) image of one fabricated device with a cloverleaf structure is shown in figure 1(a). The thickness of FGT flake in the present device is about 47 nm, which was evaluated by using the transmission electron microscopy after all the electrical measurements of the device. Anomalous Hall effect was performed in a cryostat with a temperature controlling system. To prevent the influence of spin-orbit torque effect, we detected the anomalous Hall voltage by lock-in amplifier with applying 10 μA AC current of 173 Hz. The magnetic field H is sweeping out of the FGT surface plane, as shown in figure 1(b). The magnetic field sweep rate is about 13 Oe s^{-1}, the time constant is 300 ms for reading data. The AHE signals are evaluated at 10 K for zero-field cooling (ZFC), and field cooling (FC) from 300 to 10 K.

3. Results and discussion

The AHE effect is one typical feature of the FM material. To characterize the magnetic properties of the FGT flake, we first evaluated the AHE effect by measuring anomalous Hall resistance R_{xy}, anomalous Hall voltage normalized by the applied current, as a function of external magnetic field sweeping in the out-of plane direction. The SEM and schematic of the measurement setup is shown in figures 1(a) and (b). Figure 1(c) shows the zero-field cooled AHE signal by a sweeping magnetic field from −3000 Oe to +3000 Oe and sweeping back to −3000 Oe. The square-shaped magnetic loop indicates a large perpendicular magnetic anisotropy of FGT. Here we can see the asymmetry between negative switching field (H_{CL}) and positive switching field (H_{CR}) induces an exchange-biased field $H_{ex} = (H_{CL} + H_{CR})/2 = 70$ Oe, which is a critical parameter to evaluate the EB effect. Such a spontaneous exchange-biased AHE has been reported due to the coexistence of a field-induced irreversible magnetic behavior and a spin-glass-like phase [36]. It is the first time to observe this kind of properties in the FGT flakes. To understand the underlying mechanism, we measured the FC AHE signals with applied cooling fields (H_{FC}) of ±1600 Oe from a temperature of 300 to 10 K, as shown in figures 1(d) and (e). Interestingly, the positive cooling field of 1600 Oe gives the positive EB field of 274 Oe, and the negative cooling field of −1600 Oe induces the negative exchanged bias field of −383 Oe. Those results are quite different from the conventional EB effect, where the EB field is opposite to the cooling field. This phenomenon is usually called the positive EB effect, which strongly depends on the detailed crystal structure and the interface coupling. The positive EB effect has been observed in several bi-layer systems [37–42]. Here, vdW FGT is quite different from the upon mentioned bi-layer systems, because the magnetism of FGT is highly sensitive to the local atomic arrangements or defect in a given FGT layer as well as the layer stacking configuration [43, 44]. Most recently, researchers confirmed that the Fe defect-induced Kondo hole effect or surface oxidation could induce weak coupling in the FGT layers [32, 34]. The anomalous phenomena induced by the coexistence of AFM and FM phases have been discussed with considering the existing metastable state in FGT [33, 45–47]. But the positive exchange-biased AHE can not be explained by the simple interface coupling between AFM and FM phases.

With a view to understanding such a positive EB effect, the cycle-dependence of the EB field is also studied by repeating 30 times for various cooling field at 10 K. Figure 2(a) shows the contour plots of R_{xy} as a function of cycle number N and sweeping magnetic field. The clear field switching process is observed. However, it is hard to see the standard training effect, where the coercivity and EB field gradually reduce

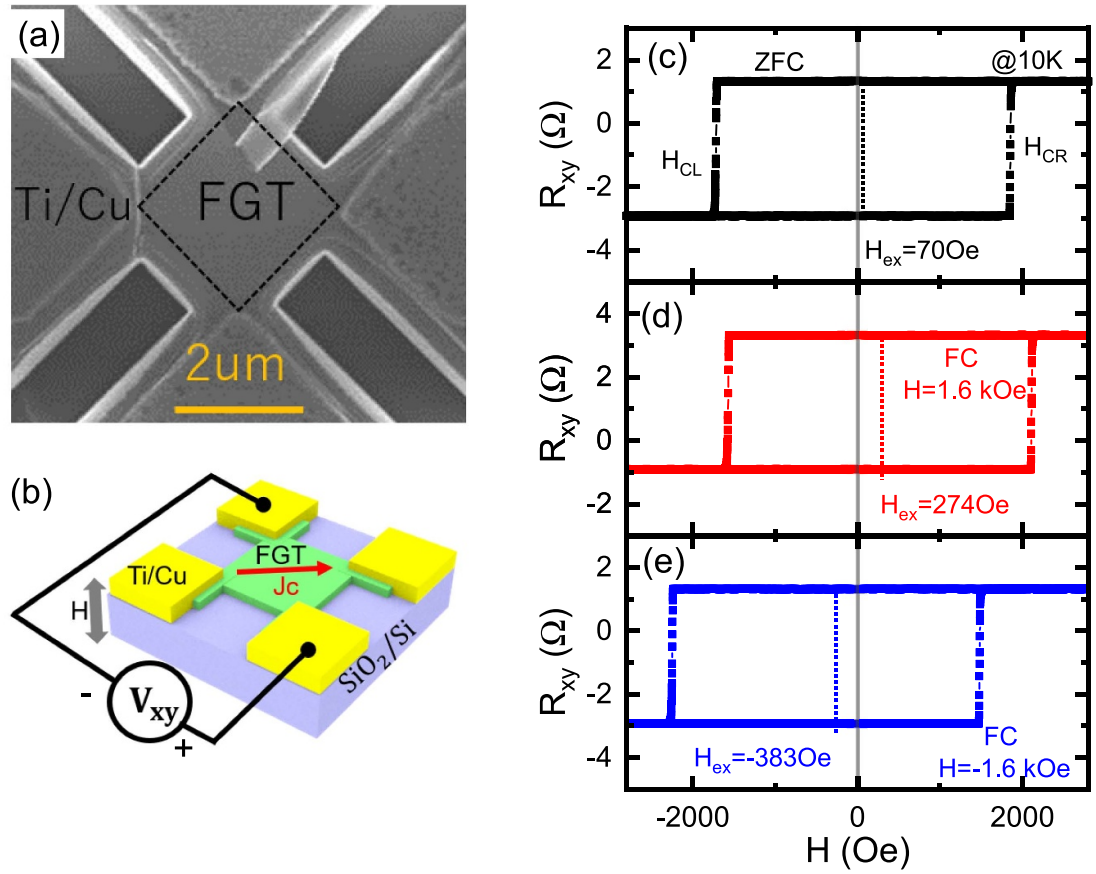

Figure 1. Characterization of EB in vdW FGT flakes. (a) Scanning electron microscopy (SEM) image of one fabricated device with cloverleaf structure. (b) The schematic of the R_{xy} measurement setup. (c)–(e) The AHE signals for zero-field cooling (ZFC) and field cooling (FC) with applied fields of ±1600 Oe from 300 to 10 K. The AHE signals are obtained by measuring R_{xy} with sweeping out-of-plane magnetic field from −3000 Oe to +3000 Oe and sweeping back to −3000 Oe. The H_{CL} and H_{CR} are the negative and positive switching fields, respectively. The EB field is defined as $H_{ex} = (H_{CL} + H_{CR})/2$. The coercivity field is $H_C = (H_{CR} - H_{CL})/2$.

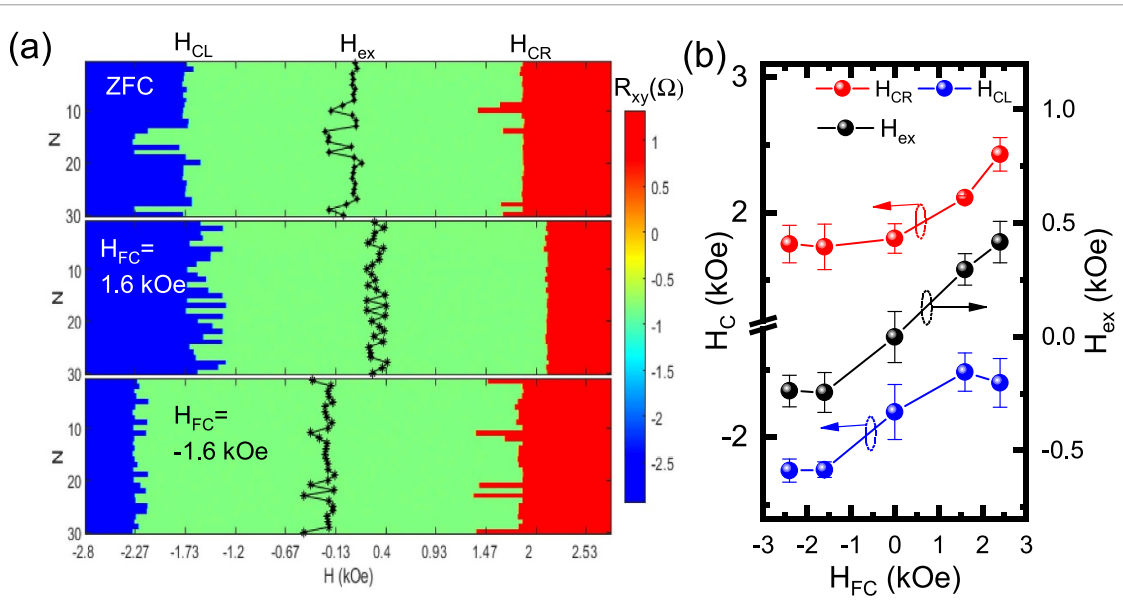

Figure 2. (a) Contour plots illustrating the magnetization switching process of anomalous Hall signal at 10 K for ZFC, FC = 1.6 kOe and FC = −1.6 kOe. The contour plot displays R_{xy} as a function of cycle number N and the sweeping magnetic field strength. One horizontal line is obtained by the averaged R_{xy} values at the same magnetic field strength with different sweeping directions for one full sweeping cycle. The boundary of the red and green regions corresponds to the negative switching field (H_{CL}). The boundary of the blue and green regions corresponds to the positive switching field (H_{CR}). The black solid line with dots corresponds to the EB field (H_{ex}). (b) Cooling field dependence of the average switching fields and the average EB fields.

during consecutive sweeping cycles. Here both the coercivity field and EB field show the hopping behavior. As we know, the standard training effect is more critical for the polycrystalline system. The origin of the training effect relates to thermally de-pinning of AFM momentum or reorientation of the coupling surface spins.

By carefully comparing the results, we can confirm that the positive cooling field will stabilize positive switching fields (H_{CR}) and vibrate negative switching fields (H_{CL}), as shown in figure 2(a). The EB fields also show the hopping behavior. The negative cooling field will give us a much more stable negative switching field. For ZFC, there is a significantly low negative switching field, which will produce the negative EB field. For understanding the absolute difference of the FC behavior, we also plotted the cooling field dependence of the average switching fields and the average EB fields shown in figure 2(b). The positive switching field H_{CR} is monotonically increasing with the cooling field, whilst H_{CL} seems already saturated in the range of cooling fields over 1.6 kOe. Nevertheless, the EB field is still almost monotonically increasing with the cooling field. The cooling-field dependence of switching fields indicates the coupling mechanism is supposed to be more complicated than one interface coupling effect for the two switching fields.

To understand this scenario, we are of the opinion that the FM phase packs the local AFM phase in such nano-flakes because of the coexisting of the AFM and FM phase in such materials [45]. The local AFM phase should have different surface coupling types with the surrounding FM phase due to the different defect densities of Fe. Here, we give a simple assumption that the coupling energy density (J_I) between the AFM phase and the surrounding FM phase are different for the two interfaces shown in figure 3(a). For the AFM/FM1 interface, the interface coupling energy density $J_{I1} = j_1\, \mathbf{S}_{AF1} \cdot \mathbf{S}_{FM1}$ is related to the up surface magnetization of AFM phase (S_{AF1}) coupling via exchange with the bottom surface magnetization of FM1 (S_{FM1}). j_1 is the exchange coupling strength between S_{AF1} and S_{FM1}. For the AFM/FM2, the interface coupling energy density J_{I2} can be expressed as $j_2\ \mathbf{S}_{AF2} \cdot \mathbf{S}_{FM2}$. Based on the Meiklejohn–Bean (MB) model [1], the switching field is simply given as follows:

$$H_{CL} = -\frac{K_u}{\mu_0 M_S} - \frac{j_1 \mathbf{S}_{AF1} \cdot \mathbf{S}_{FM1}}{\mu_0 \mathbf{M}_{FM1} t_{FM1}} - \frac{j_2 \mathbf{S}_{AF2} \cdot \mathbf{S}_{FM2}}{\mu_0 \mathbf{M}_{FM2} t_{FM2}} \quad (1)$$

$$H_{CR} = \frac{K_u}{\mu_0 M_S} - \frac{j_1 \mathbf{S}_{AF1} \cdot \mathbf{S}_{FM1}}{\mu_0 \mathbf{M}_{FM1} t_{FM1}} - \frac{j_2 \mathbf{S}_{AF2} \cdot \mathbf{S}_{FM2}}{\mu_0 \mathbf{M}_{FM2} t_{FM2}} \quad (2)$$

where, K_u is the anisotropy energy of FM layers, the M_S is the saturation of the FM layer, $\mathbf{M}_{FM1} = M_S\ \mathbf{m}_1$ and $\mathbf{M}_{FM2} = M_S\ \mathbf{m}_2$. $\mathbf{m}_1$ and $\mathbf{m}_2$ are the unit vector for magnetic momentum of FM1 and FM2, respectively. t_{FM1} and t_{FM2} are the thickness for the FM1 and FM2 layer, respectively. In the following analysis, we assume $t_{FM1} = t_{FM2} = t_{FM}$.

The interface coupling energy density is also affected by the anisotropy energy and total Zeeman energy of the surface magnetization with the cooling field. When the temperature is below the freezing temperature of the AFM phase for zero cooling field, the S_{AF} will be a metastable state because of the competition of anisotropy strength of AFM and surface exchange coupling strength. So the interface coupling energy density may positive or negative. If the total value of the two interface coupling energy density ($J_I = J_{I1} + J_{I2}$) is not zero, the spontaneous EB effect will happen even for the ZFC. For the negative total interface coupling energy density $J_I < 0$, a positive EB field will be created. The positive value of J_I will create a negative bias field. The interface coupling energy density also depends on the cooling field-induced Zeeman energy. The Zeeman energy of the interface magnetization in the cooling field favors parallel alignment of S_{AF} with respect to S_{FM}. The AFM coupling supports antiparallel alignment of the S_{AF} with respect to the S_{FM}. The total result of this fight between these two energies will determine the future of the EB field.

The figure 3(b) displays the situation of a large positive FC ($\mu_0 H_{FC} M_s t_{FM} > \mid j_1 \mathbf{S}_{FM1} \mid, \mid j_2 \mathbf{S}_{FM2} \mid$). The Zeeman energy overcomes the AFM exchange coupling giving rise to a parallel alignment of S_{AF} and S_{FM} for two interfaces during the field-cooling process. For the AFM exchange coupling of interface 2 ($j_2 < 0$), the positive S_{SAF2} will be much stable due to the enhancement of anisotropy strength during the positive cooling field. If interface 1 holds the FM exchange coupling ($j_1 > 0$), the S_{SAF1} will be in a metastable state because of the reduction of anisotropy strength during the positive cooling field. The positive EB indicates that $\mid J_{I1} \mid$ is less than $\mid J_{I2} \mid$. In addition, the $\mathbf{S}_{SAF1}$ will be easily reversal by applying one negative field shown in figure 3(c). As a result, the $J_1 \mathbf{S}_{SAF1}$ will change the sign resulting in the modification of J_I. Hence, we can observe the vibrated EB field as a function of sweeping cycles. Due to the anisotropy of the AFM phase, we believe that the negative cooling field will not produce the same amplitude of S_{SAF1} and S_{SAF2} as the positive cooling field. As a result, the exchange bias behavior will exhibit asymmetry cooling field dependence.

For intuitionally understanding the vibration of EB, we demonstrate the magnetization process for exchanged-bias anomalous Hall signal with positive cooling field shown in figure 3(d) under two cycles. The initial state 1–1 contains two surface coupling interfaces. When the negative field breaks the S_{SAF1} state, the S_{SAF1} could be reversed shown in 1–2 state. The probability of the reversion of positive S_{SAF1} to

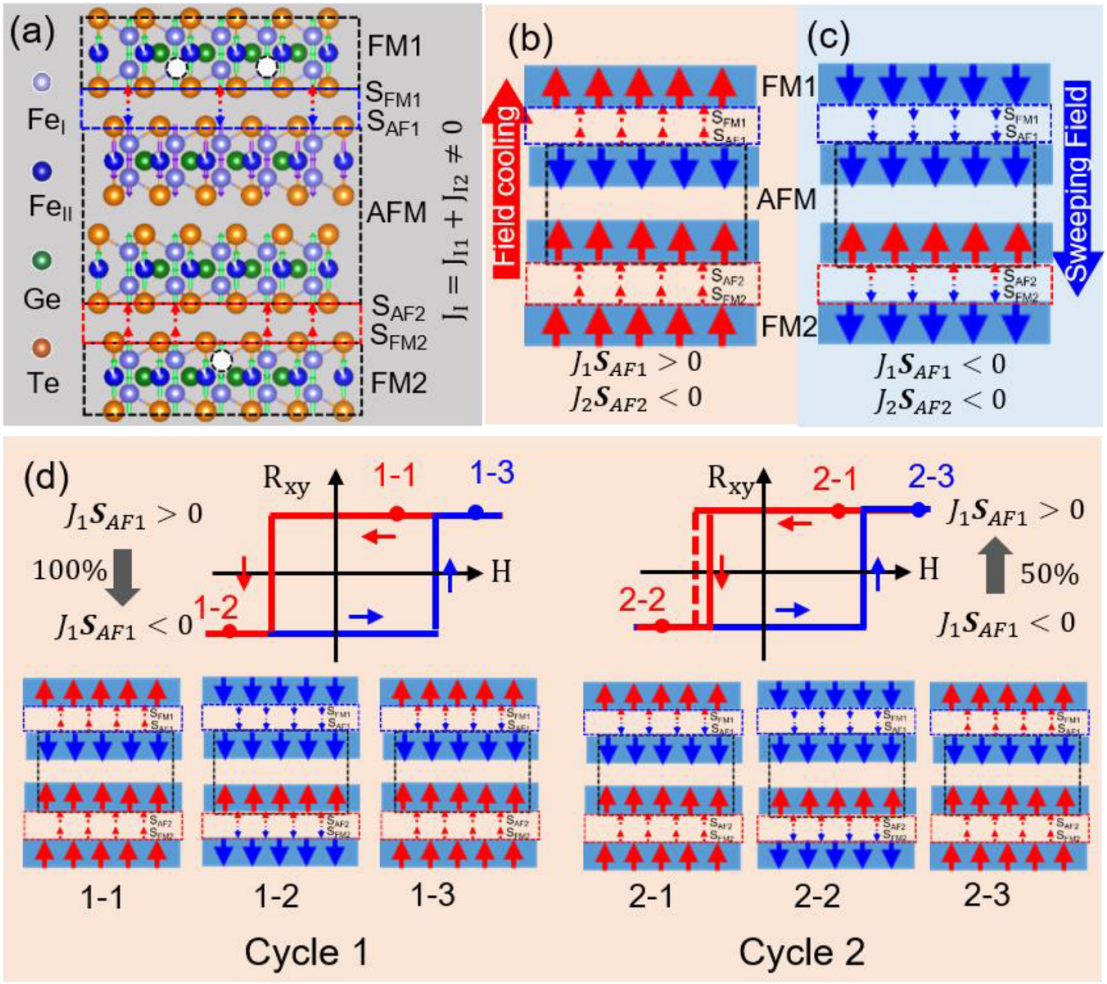

Figure 3. (a) Schematic picture of one unit cell's magnetic configuration for the coupling model. The magnetic configurations of the AFM phase (center of black dashed box) are sandwiched by the FM phase. The dashed arrows between the layers indicate the surface magnetization of AFM phase (S_{AF}) and surface magntization of FM (S_{FM}). (b) Schematic picture of the magnetic configuration for positive field cooling (PFC). (c) The magnetic configuration for applying negative field after PFC. The positive S_{AF1} becomes negative S_{AF1} during the applying negative field. The S_{AF2} does not alter the magnetization direction. (d) Magnetic hysteresis curves with the corresponding magnetic configurations for two cycles with the reversion of S_{AF1}.

the negative S_{SAF1} state is 100% under the negative external magnetic field. Applying the positive field also has a chance to reverse negative S_{SAF1} to positive S_{SAF1} state again. Moreover, the possibility is about 50% based on the number of hopping switching in the experimental results. If the positive field does not change the S_{SAF1} state at the end of the first cycle, the absolute value of total interface coupling energy density will be higher for 2–1 sate in cycle 2. This will make the negative switching field come earlier than the first cycle. The positive switching field will not change because the 2–2 state is the same as 1–2. So the positive switching field is very stable. The magnetization also can become 2–3 state due to the reversion of the negative S_{SAF1} state during the magnetization switching by sweeping the magnetic field in the positive direction. Then it will repeat cycle 1. Moreover, we can obtain the EB fields for cycle 1 $\left(-\frac{j_2 S_{AF2} S_{FM2}}{\mu_0 M_{FM} t_{FM}}\right)$ and $\left(-\frac{-j_1 S_{AF1} S_{FM1} + j_2 S_{AF2} S_{FM2}}{\mu_0 M_{FM} t_{FM}}\right)$ for cycle 2. This process can help us to understand the hopping behavior of the EB field clearly.

4. Microspin simulation

To deeply understand this upon the model in FGT, we calculated the exchange-biased magnetic hysteresis loops using the microspin simulation with Mumax3 [48, 49]. The AFM layer is covered by two FM layers in the simulation, as shown in figure 3(b). Both saturation magnetization of FM and AFM layer are $M_s = 3.76 \times 10^5$ A m^{-1}. The magnetic anisotropy energy density of FM and AFM are $K_u = 5.1 \times 10^5$ J m^{-2} and $K_u = 1.0 \times 1^7$ J m^{-2} [23, 32]. The interlayer coupling energy density of stable surface magnetization of AFM phase $J_{I2} = -2.9 \times 10^{-4}$ J m^{-2} and frustrated surface magnetization of AFM phase $J_{I1} = 2.9 \times 10^{-4}$ J m^{-2} are evaluated from maximum and minimum values of

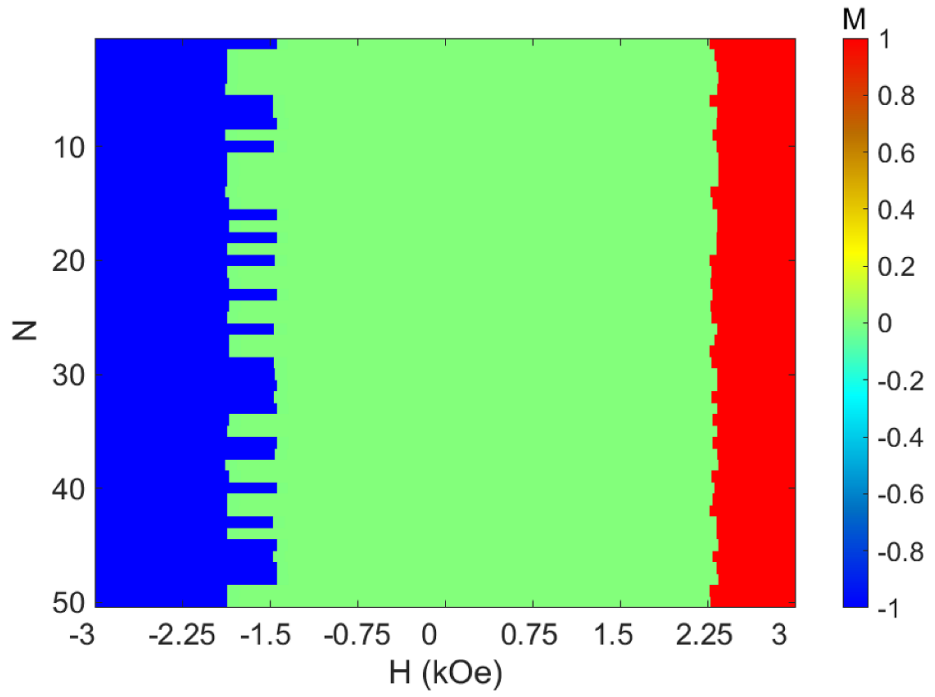

Figure 4. Contour plots illustrate the magnetization switching process with 50 sweeping cycles. The contour plot displays magnetic momentum as a function of cycle number N and the sweeping magnetic field strength. One horizontal line is obtained by the averaged M values at the same magnetic field strength with different sweeping directions for one full sweeping cycle.

EB field ($H_{ex}^{max} = 400$ Oe and $H_{ex}^{min} = 200$ Oe) at $H_{FC} = 1.6$ kOe with the Meiklejohn–Bean model [1]. We calculate 50 M-H loops and give the contour plots illustrating the magnetization switching process in figure 4. The random hopping of the switching fields is also clearly obtained. We can reproduce the experimental results based on two different coupling surfaces model in AFM and FM states.

5. Conclusion

In summary, we first observed the positive exchange-biased anomalous Hall effect with a hopping switching behavior in FeGeTe nano-flakes. The exchange-biased field is monotonically tunable by the cooling field. Furthermore, the coexistence of stable and frustrated surface magnetization of the AFM phase gives a good explanation of the unconventional exchange-biased effect. Our findings may provide essential insights into the spin coupling mechanism between the vdW magnetic layers.

Data availability statement

The data that support the findings of this study are available upon reasonable request from the authors.

Acknowledgments

This work is partially supported by National Key Research Program of China (Grant No. 2017YFA0206202), International Postdoctoral Exchange Fellowship Program (20190083), ARC Centre of Excellence in Future Low-Energy Electronics Technologies (No. CE170100039), JSPS Program for Grant-in-Aid for Scientific Research (S)(21H05021), that for Challenging Exploratory Research (17H06227) and JST CREST (JPMJCR18J1).

ORCID iDs

Shaojie Hu https://orcid.org/0000-0003-3799-972X
Kohei Ohnishi https://orcid.org/0000-0002-8148-5366
Xiaolin Wang https://orcid.org/0000-0003-4150-0848
Takashi Kimura https://orcid.org/0000-0002-1253-2130

References

[1] Meiklejohn W H and Bean C P 1956 New magnetic anisotropy *Phys. Rev.* **102** 1413–4
[2] Nogués J and Schuller I K 1999 Exchange bias *J. Magn. Magn. Mater.* **192** 203–32
[3] Berkowitz A E and Takano K 1999 Exchange anisotropy—a review *J. Magn. Magn. Mater.* **200** 552–70
[4] Shaojie H, Kiseki K, Yakata S and Kimura T 2012 Ferromagnetic resonance in exchange-coupled NiFe/FeMn films and its control *IEEE Trans. Magn.* **48** 2889–91
[5] van der Zaag P J, Wolf R M, Ball A R, Bordel C, Feiner L F and Jungblut R 1995 A study of the magnitude of exchange biasing in [111] Fe_3O_4/CoO bilayers *J. Magn. Magn. Mater.* **148** 346–8

[6] Tokunaga T, Taguchi M, Fukami T, Nakaki Y and Tsutsumi K 1990 Study of interface wall energy in exchange-coupled double-layer film *J. Appl. Phys.* **67** 4417–9

[7] Cain W C and Kryder M H 1990 Investigation of the exchange mechanism in NiFe-TbCo bilayers *J. Appl. Phys.* **67** 5722–4

[8] Freitas P P, Leal J L, Melo L V, Oliveira N J, Rodrigues L and Sousa A T 1994 Spin-valve sensors exchange-biased by ultrathin TbCo films *Appl. Phys. Lett.* **65** 493–5

[9] Radu F, Abrudan R, Radu I, Schmitz D and Zabel H 2012 Perpendicular exchange bias in ferrimagnetic spin valves *Nat. Commun.* **3** 715

[10] Gökemeijer N J, Ambrose T and Chien C L 1997 Long-range exchange bias across a spacer layer *Phys. Rev. Lett.* **79** 4270–3

[11] Bruno P and Chappert C 1991 Oscillatory coupling between ferromagnetic layers separated by a nonmagnetic metal spacer *Phys. Rev. Lett.* **67** 1602–5

[12] Bruno P and Chappert C 1992 Ruderman–Kittel theory of oscillatory interlayer exchange coupling *Phys. Rev.* B **46** 261–70

[13] Ali M, Adie P, Marrows C H, Greig D, Hickey B J and Stamps R L 2007 Exchange bias using a spin glass *Nat. Mater.* **6** 70–75

[14] Gruyters M 2005 Spin-glass-like behavior in CoO nanoparticles and the origin of exchange bias in layered CoO/ferromagnet structures *Phys. Rev. Lett.* **95** 10–13

[15] Yuan F T, Lin J K, Yao Y D and Lee S F 2010 Exchange bias in spin glass (FeAu)/NiFe thin films *Appl. Phys. Lett.* **96** 2010–3

[16] Rui W B *et al* 2014 Asymmetric exchange bias training effect in spin glass (FeAu)/FeNi bilayers *Chin. Phys.* B **23**

[17] Rui W B, Hu Y, Du A, You B, Xiao M W, Zhang W, Zhou S M and Du J 2015 Cooling field and temperature dependent exchange bias in spin glass/ferromagnet bilayers *Sci. Rep.* **5** 13640

[18] Sahoo R C, Takeuchi Y, Ohtomo A and Hossain Z Exchange bias and spin glass states driven by antisite disorder in the double perovskite compound $LaSrCoFeO_6$ *Phys. Rev.* B **100** 214436

[19] Lachman E, Murphy R A, Maksimovic N, Kealhofer R, Haley S, McDonald R D, Long J R and Analytis J G 2020 Exchange biased anomalous Hall effect driven by frustration in a magnetic kagome lattice *Nat. Commun.* **11** 1–8

[20] Maniv E *et al* 2021 Exchange bias due to coupling between coexisting antiferromagnetic and spin-glass orders *Nat. Phys.* **17** 525–30

[21] Gong C *et al* 2017 Discovery of intrinsic ferromagnetism in two-dimensional van der Waals crystals *Nature* **546** 265–9

[22] Huang B *et al* 2017 Layer-dependent ferromagnetism in a van der Waals crystal down to the monolayer limit *Nature* **546** 270–3

[23] Deng Y *et al* 2018 Gate-tunable room-temperature ferromagnetism in two-dimensional Fe_3GeTe_2 *Nature* **563** 94–99

[24] Fei Z *et al* 2018 Two-dimensional itinerant ferromagnetism in atomically thin Fe_3GeTe_2 *Nat. Mater.* **17** 778–82

[25] Zhu R *et al* 2020 Exchange bias in van der Waals $CrCl_3/Fe_3GeTe_2$ heterostructures *Nano Lett.* **20** 5030–5

[26] Srivastava P K *et al* 2020 Exchange bias effect in ferro-/antiferromagnetic van der Waals heterostructures *Nano Lett.* **20** 3978–85

[27] Guojing H *et al* 2020 Antisymmetric magnetoresistance in a van der Waals antiferromagnetic/ferromagnetic layered $MnPS_3/Fe_3GeTe_2$ stacking heterostructure *ACS Nano* **14** 12037–44

[28] Zhang L *et al* 2020 Proximity-coupling-induced significant enhancement of coercive field and Curie temperature in 2D van der Waals heterostructures *Adv. Mater.* **32** 2002032

[29] Yu Z *et al* 2021 Exchange bias and spin–orbit torque in the Fe_3GeTe_2-based heterostructures prepared by vacuum exfoliation approach *Appl. Phys. Lett.* **118** 262406

[30] Dai H, Cheng H, Cai M, Hao Q, Xing Y, Chen H, Chen X, Wang X and Han J-B 2021 Enhancement of the coercive field and exchange bias effect in $Fe_3GeTe_2/MnPX_3$ (X = S and Se) van der Waals heterostructures *ACS Appl. Mater. Interfaces* **13** 24314–20

[31] Zheng G *et al* 2020 Gate-tuned interlayer coupling in van der Waals ferromagnet Fe_3GeTe_2 nanoflakes *Phys. Rev. Lett.* **125** 47202

[32] Gweon H K *et al* 2021 Exchange bias in weakly interlayer-coupled van der Waals magnet Fe_3GeTe_2 *Nano Lett.* **21** 1672–8

[33] Zhang Y *et al* 2018 Emergence of Kondo lattice behavior in a van der Waals itinerant ferromagnet, Fe_3GeTe_2 *Sci. Adv.* **4** eaao6791

[34] Zhao M *et al* 2021 Kondo holes in the two-dimensional itinerant Ising ferromagnet Fe_3GeTe_2 *Nano Lett.* **21** 6117–23

[35] Park T E *et al* 2021 Néel-type skyrmions and their current-induced motion in van der Waals ferromagnet-based heterostructures *Phys. Rev.* B **103** 104410

[36] Wang B M, Liu Y, Ren P, Xia B, Ruan K B, Yi J B, Ding J, Li X G and Wang L 2011 Large exchange bias after zero-field cooling from an unmagnetized state *Phys. Rev. Lett.* **106** 077203

[37] Nogués J, Lederman D, Moran T J and Schuller I K 1996 Positive exchange bias in FeF_2-Fe bilayers *Phys. Rev. Lett.* **76** 4624–7

[38] Nogués J, Leighton C and Schuller I K 2000 Correlation between antiferromagnetic interface coupling and positive exchange bias *Phys. Rev.* B **61** 1315–7

[39] Yang D Z, Du J, Sun L, Wu X S, Zhang X X and Zhou S M 2005 Positive exchange biasing in GdFe/NiCoO bilayers with antiferromagnetic coupling *Phys. Rev.* B **71** 144417

[40] Ohldag H, Shi H, Arenholz E, Stöhr J and Lederman D 2006 Parallel versus antiparallel interfacial coupling in exchange biased Co/FeF_2 *Phys. Rev. Lett.* **96** 027203

[41] Suszka A K, Idigoras O, Nikulina E, Chuvilin A and Berger A 2012 Crystallography-driven positive exchange bias in Co/CoO bilayers *Phys. Rev. Lett.* **109** 22–26

[42] Gilbert D A *et al* 2016 Controllable positive exchange bias via redox-driven oxygen migration *Nat. Commun.* **7** 11050

[43] Kong X 2020 Interlayer magnetism in $Fe_{3-x}GeTe_2$ *Phys. Rev. Mater.* **4** 094403

[44] May A F, Du M-H, Cooper V R and McGuire M A 2020 Tuning magnetic order in the van der Waals metal Fe_5GeTe_2 by cobalt substitution *Phys. Rev. Mater.* **4** 074008

[45] Yi J, Zhuang H, Zou Q, Wu Z, Cao G, Tang S, Calder S A, Kent P R, Mandrus D and Gai Z 2016 Competing antiferromagnetism in a quasi-2D itinerant ferromagnet: Fe_3GeTe_2 *2D Mater.* **4** 011005

[46] Jang S W, Yoon H, Jeong M Y, Ryee S, Kim H S and Han M J 2020 Origin of ferromagnetism and the effect of doping on Fe_3GeTe_2 *Nanoscale* **12** 13501–6

[47] Seo J *et al* 2020 Tailoring high-TN interlayer antiferromagnetism in a van der Waals itinerant magnet (arXiv:2004.12650)

[48] Vansteenkiste A, Leliaert J, Dvornik M, Helsen M, Garcia-Sanchez F and Bartel V W 2014 The design and verification of MuMax3 *AIP Adv.* **4** 107133

[49] De Clercq J, Vansteenkiste A, Abes M, Temst K and Bartel V W 2016 Modelling exchange bias with $MuMax^3$ *J. Phys. D: Appl. Phys.* **49** 435001